

Mach-Zehnder Interferometer Based on All-fiber Multimode Interference Device for DPSK Signal Demodulation

Xiaoyong Chen⁽¹⁾, David Garcia⁽¹⁾, Alfredo Martín Minguez⁽²⁾, Paloma R. Horche⁽¹⁾
 xiaoyong.chen@alumnos.upm.es, David.garcia.regodon@alumnos.upm.es, alfredo.martin@upm.es,
 phorche@tfo.upm.es

⁽¹⁾ Departamento de Tecnología Fotónica y Bioingeniería

⁽²⁾ Departamento de Tecnología Electrónica

Escuela Técnica Superior de Ingenieros de Telecomunicación, Universidad Politécnica de Madrid, Avda. Complutense 30, Madrid - 28040.

Abstract- Differential Phase Shift Keying (DPSK) modulation format has been shown as a robust solution for next-generation optical transmission systems. One key device enabling such systems is the delay interferometer, converting the signal phase information into intensity modulation to be detected by the photodiodes. Usually, Mach-Zehnder interferometer (MZI) is used for demodulating DPSK signals. In this paper, we developed an MZI which is based on all-fiber Multimode Interference (MI) structure: a multimode fiber (MMF) located between two single-mode fibers (SMF) without any transition zones.

The standard MZI is not very stable since the two beams go through two different paths before they recombine. In our design the two arms of the MZI are in the same fiber, which will make it less temperature-sensitive than the standard MZI. Performance of such MZI will be analyzed from transmission spectrum. Finally such all-fiber MI-based MZI (MI-MZI) is used to demodulate 10 Gbps DPSK signals. The demodulated signals are analyzed from eye diagram and bit error rate (BER).

I. INTRODUCTION

Differential Phase Shift Keying (DPSK) is an attractive modulation format for next-generation optical transmission systems since it exhibits high tolerance to chromatic dispersion (CD) and robustness to nonlinear effects. Besides these advantages, it also offers an improved receiver sensitivity by balanced detection. In DPSK communications, one key device which is able to convert the differential phase information into intensity information to be detected by the photodiodes is a delay interferometer, such as Mach-Zehnder interferometer (MZI). Usually, MZI is used for demodulating DPSK signals because of its simple structure. In recent years, all-fiber MZI is proposed to take place of the standard MZI for improving the performance. It is not only used for measurement of temperature, pressure, flatness of plane optical plates, thickness of thin film, coherence length of a laser, but also used in optical communication, such as DPSK demodulator [1]. However, in the DPSK demodulation scheme proposed in ref. [1], there is one problem of stability due to the two beams go through two different paths and the effect, which is generated from temperature and pressure, on both arms is different. For further improving the performance of all-fiber MZI, several schemes are proposed recently. In [2]

a photonic crystal fiber (PCF) based MZI for DPSK signal demodulation is presented. In this scheme the device is fabricated by mismatch splicing of a PCF with standard single mode fibers (SMFs). In [3] a multimode fiber (MMF) based interferometer for differential phase demodulation is proposed.

All-fiber-based MZI is attractive since it is low-cost and easy implementation. In this paper we will present an all-fiber Multimode Interference-based MZI (MI-MZI) for DPSK signals demodulation. Performance of the MI-MZI is study deeply from transmission spectrum based on a theoretical study and experiments. Finally, a DPSK demodulator based MI-MZ will also be presented and discussed from theory and simulations.

The paper is organized as the following. The theory of MI-MZI will be presented in section 2. Experimental setup and results will be shown and discussed in section 3. In section 4 we will present the simulation structure for demodulating DPSK signals and discuss the simulation results. Finally, the conclusions will be presented in section 5.

II. THEORY

The modal interference process is a well known phenomenon and it had been studied by several authors [3-9]. Based on this principle we can make an interferometer as a

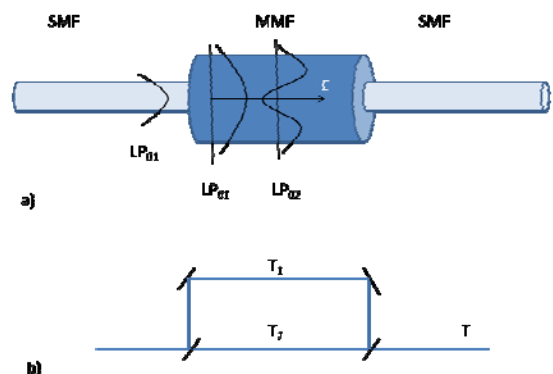


Fig 1 Comparison between MI-MZI structure (a) and a standard MZI (b)

MZI. The structure of the MI-MZI is shown in Fig. 1a where only core fibers are drawn. The structure is composed of a multimode region located between two single-mode regions without any transition zones. This passive device has been made with just a multimode fiber (50/125 μm) spliced between two single-mode fibers (9/125 μm). Moreover, a simple connector (with a matched liquid index to avoid reflection interfaces) can be employed to couple single-mode and multimode fibers without any fusion. Both configurations have been employed by us and similar results have been obtained [5, 7].

Since the central region of a MI-MZI is multimode, coupling between the LP_{01} single-mode fiber and all the other modes of the multimode fiber is possible. However, coupling occurs preferentially between the LP_{01} mode and the LP_{02} mode since both modes have similar azimuthal symmetry and the phase mismatch is minimized. Since excited fundamental (LP_{01}) and first order symmetry (LP_{02}) modes are propagating in the multimode fiber with different phase constant, these modes interfere with each other along the direction of propagation. The light power coupled into the SMF-output fiber depends on the relative phase difference at the end of the multimode fiber (L).

Compared with the standard MZI (as shown in Fig. 1b) which obtains a time delay through a physical path length difference, the MI-MZI obtains a time delay from time difference for both modes passing through the MMF transmission path.

The number of modes that a fiber can support is related to the V -parameter of the fiber. The V -parameter is defined as [10]:

$$V = \frac{2\pi a}{\lambda} \sqrt{n_{core}^2 - n_{clad}^2} \quad (1)$$

where a is the core radius, λ is the wavelength in vacuum, n_{core} is the maximum refractive index of the core and n_{clad} is the refractive index of the cladding. Ideally, in our scheme we want to have only two circular-symmetric modes.

The MMF we will use has a w-type index profile shown in Fig. 2. This refractive index dip decreases power coupling from input mode to zero-order mode and increases coupling to next-order symmetric modes. This effect causes w-type index profile to have an extinction ratio higher than step index profile. Also, with this kind of fibers we can achieve a better LP_{01} - LP_{02} modes beating because the non symmetrical modes, such as modes LP_{11} and LP_{21} , are less coupling.

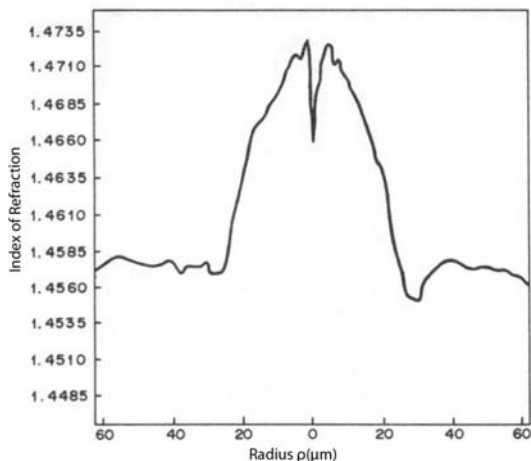


Fig. 2 Refractive index profile of a w-type fiber

The transmission is periodic with respect to the frequency and is usually represented by a comb-filtering spectrum as depicted, i.e., in Figs. 4-6. The spacing $\Delta\lambda$ between the adjacent constructive peaks (destructive valleys) can be written as [11]:

$$\Delta\lambda = \frac{\lambda^2}{|n_{01} - n_{02}|L} = \frac{2\pi\lambda}{|\beta_{01} - \beta_{02}|L} = \frac{\lambda z_b}{L} \quad (2)$$

Where n_{01} and n_{02} are the effective index of refraction for modes LP_{01} and LP_{02} respectively; $z_b = \frac{2\pi}{|\beta_{01} - \beta_{02}|}$ [12] is the beat length of the MMF.

From (2) we can see that it is possible to adjust the separation between peaks by adjusting the length of the MMF. Using these properties we can do a transmission spectrum very similar to a standard MZI spectrum.

The propagation constant of the two beating modes can be written as:

$$\beta_{01} - \beta_{02} = \frac{\lambda}{4\pi a^2 n_{core}} (U_{01}^2 - U_{02}^2) \quad (3)$$

where

$$U_{01} = 2.405 e^{-1/V} \quad \text{for the mode } LP_{01} (\text{HE}_{11})$$

$$U_{02} = 5.520 e^{-1/V} \quad \text{for the mode } LP_{02} (\text{HE}_{12})$$

The transmission spectrum of this MI-MZI can be described as follows:

$$T = T_1 + T_2 + 2\sqrt{T_1 T_2} \cos(\varphi) \quad (4)$$

$$\varphi = \int_0^L \Delta\beta(z) dz = L\Delta\beta_{12} \quad (5)$$

where T_1 and T_2 are the intensity of the two modes LP_{01} and LP_{02} , respectively; L is the length of the MMF; $\Delta\beta_{12}$ is the difference between the propagation constant of the modes LP_{01} and LP_{02} . The operation principle is based on standard MZI with the LP_{01} and LP_{02} modes taken as the two interference arms.

Also, combining with the Eq. (2), the time delay between two modes can be defined by the following function:

$$\Delta t = \frac{L}{c/n_{01}} - \frac{L}{c/n_{02}} = \frac{\Delta n L}{c} = \frac{\lambda^2}{cL\Delta\lambda} \quad (6)$$

Here we define another parameter which is called delay coefficient Δd . It is corresponding to the time delay in a one-meter MMF. It can be described as:

$$\Delta d = \frac{\Delta t}{L} = \frac{\Delta n}{c} = \frac{\lambda^2}{cL\Delta\lambda} \quad (7)$$

We can see that the delay time of the MI-MZI is only determined by the effective index difference Δn between two modes, which is governed by the MMF structure.

III. EXPERIMENTAL RESULTS OF THE MI-MZI

The experimental setup using for the measurements is shown in Fig. 2. For testing the transmission spectrum of the MI-MZI, a white light is used as light source because it has a very wide spectrum from 0.4 μm to 1620 μm . The MMF used in the experiment has the core and clad diameter of 50 μm and 125 μm , respectively. The numerical aperture (NA) is 0.22. The refraction index of core and clad is 1.4730 and 1.4567,

respectively. Finally a spectrum analyzer is used to observe and record the transmission spectrum.

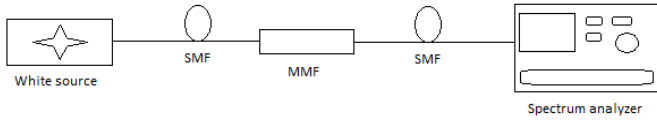


Fig. 3 Experimental setup to measure wavelength transmission

In order to observe the spacing $\Delta\lambda$ between adjacent constructive peaks (destructive valleys) changing with the length of MMF, we use different length of MMF (12cm, 18.9cm and 24cm). The experimental results are shown in Figs. 4-6. Fig. 4 (a) shows the transmission spectrum of the MI-MZI with MMF length of 12cm and the line (b) shows the spectral respond of the white source used in the experimental setup. As can be seen, it decreases for $\lambda > 1400\text{nm}$, this causes lower amplitude oscillation for wavelengths greater than that.

The experimental results clearly show that when the length of MMF increases, the spacing $\Delta\lambda$ decreases. These results are in agreement with the theory which requires that the spectral period should be inversely proportional to the length of the MMF. As it can be seen in Figs. 4-6, the power oscillation has a certain modulation indicating the existence of more than two modes. Numerical calculations have indicated that four of the modes carrying most of the energy. Because every pair of modes has a different propagation constant difference, different oscillation amplitudes are obtained.

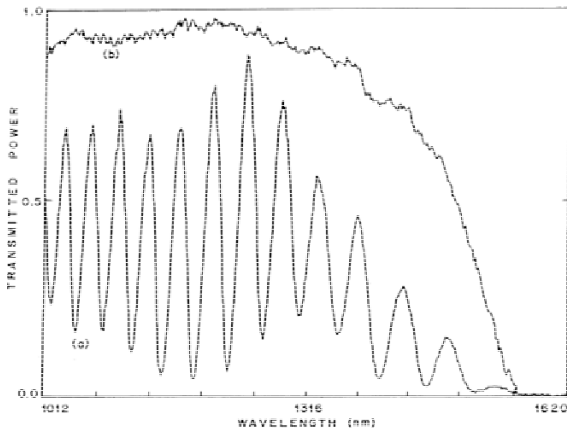


Fig.4 (a) Transmission spectrum of MI-MZI with MMF length of 12 cm; (b) Transmission spectrum of white source

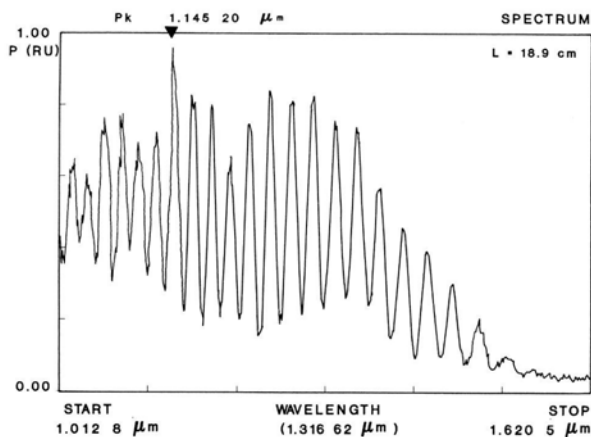


Fig. 5 Transmission spectrum of MI-MZI with MMF length of 18.9 cm

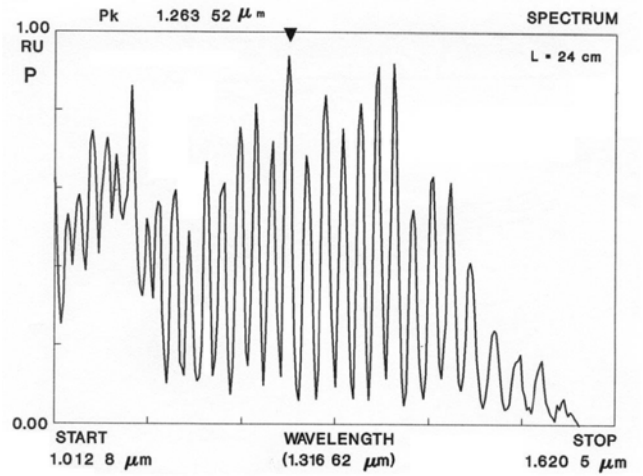


Fig. 6 Transmission spectrum of MI-MZI with MMF length of 24 cm

IV. MI-MZI FOR DPSK SIGNALS DEMODULATION

Considering the MI-MZI as a delay line interferometer (DLI), it can be directly used for demodulating DPSK signals. A basic diagram of MI-MZI for DPSK signals demodulation is shown in Fig. 7a. And we follow it to build a simulation system as shown in Fig. 7b.

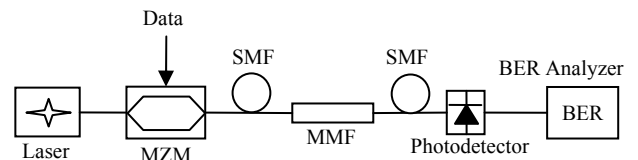


Fig. 7a Principle of MI-MZI for DPSK signals demodulation. MZM: Mach-Zehnder modulator; BER: bit error rate

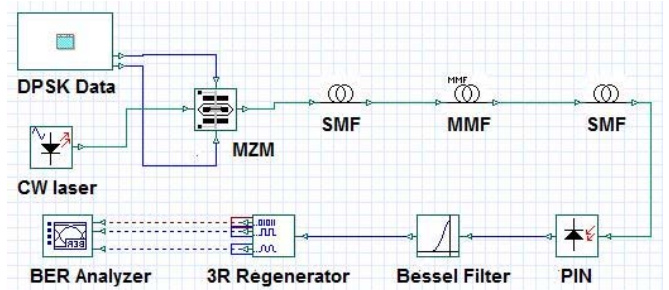


Fig. 7b Simulation system of MI-MZI for DPSK signals demodulation

In the simulation a tunable laser is used to align the source with the transmission peak of the interferometer. A Mach-Zehnder modulator (MZM), which is driven by a 10Gbps DPSK data stream, is used to modulate the light to generate a 10Gbps optical NRZ-DPSK signal. The simulated MMF has the same parameters as the MMF used in the experiment, with length of 28.7m to generate 100ps delay between the two modes. Finally, a photodiode is used to receive the demodulated signal and a bit error rate (BER) analyzer is used to analyze the performance of the received signal.

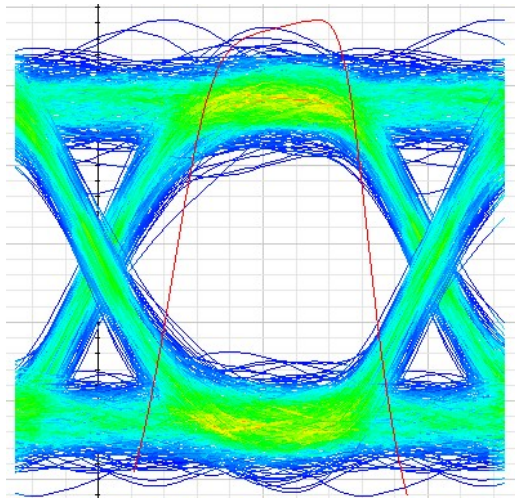


Fig. 8a Eye diagram

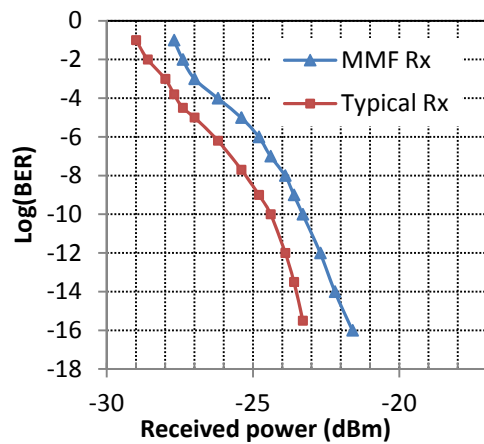


Fig. 8b BER vs Received power

The simulation results are shown in Fig. 8. The eye diagram shows a relatively open intensity eye which can provide error-free operation. Fig. 8b shows the BER of the received signal as a function of the received power. We can see that the sensitivity of the MMF receiver is about -22dBm at a BER of 10^{-15} and about -23.5dBm at a BER of 10^{-9} . Compared with the typical DLI DPSK receiver which is built with two fiber couplers and has the sensitivity of -23.6dBm at a BER of 10^{-15} and -24.8dBm at a BER of 10^{-9} , there is about 1.4 ± 0.2 dB power penalty by using the MMF receiver. This penalty is caused by several aspects, such as the loss in the MMF, and the low extinction ratio (ER) of the interference between the two modes. The ER depends on two factors: the first one is the coupling efficiency between the mode LP_{01} in the SMF and the modes LP_{01} and LP_{02} in the MMF. From (4) we know that only when the powers of the LP_{01} and LP_{02} modes are the same, the transmission spectrum of the MI-MZI would reach the highest ER. The second factor is the non symmetrical modes excited in the MMF. Although the MMF with w-type index profile decreases power coupling from input mode to LP_{01} mode and increases coupling to LP_{02} and reduce the non symmetrical modes coupling, there are still non symmetrical modes, such as LP_{11} and LP_{21} , propagating in the MMF, which would decrease ER and lead to power penalty.

V. Conclusion

We have demonstrated a MI-MZI, which is based on a MMF between two SMFs. In this structure the excited fundamental (LP_{01}) and first order symmetry (LP_{02}) modes are propagating in the multimode fiber with different phase constants. These modes interfere with each other along the direction of propagation and the light power coupled into the SMF-output fiber depends on the relative phase difference at the end of the multimode fiber (L). So we can obtain an interferometer pattern at the exit of the second section of SMF. The results of an experimental verification are in agreement with the theory. Also, a simulation for using the MI-MZI to demodulate a DPSK signal is done; the simulation results show that MMF receiver has similar performance as the typical DLI DPSK receiver [13] with a 1.4 ± 0.2 dB power penalty.

Since the design of MI-MZI is low cost and easily manufactured, it will be used widely in many optical applications in the future, such as using as filters or temperature sensors. Moreover, with the proper design it also can be used as WDM multiplex and demultiplex.

ACKNOWLEDGMENTS

The authors would like to acknowledge support from the China Scholarship Council (CSC).

REFERENCES

- [1] F. Séguin, and F. Gonthier, "Tuneable All-Fiber Delay-Line Interferometer for DPSK Demodulation," in *Tech. Dig. OFC'2005*, pp: OFL5 (2005)
- [2] Jiangbing Du, Yongheng Dai, Gordon K. P. Lei, Weijun Tong, and Chester Shu, "Photonic crystal fiber based Mach-Zehnder interferometer for DPSK signal demodulation", *Optics Express*, Vol. 18, No. 8, pp: 7917-7922 (2010)
- [3] Yannick Keith Lize, Robert Gomma and Raman Kashyap, "Low-cost multimode fiber Mach-Zehnder interferometer for differential phase demodulation", in *proc. SPIE 2006*, San Diego, USA, August (2006)
- [4] Marek Blahut, Damian Kasprzak, "Multimode interference structures – properties and applications", *Optica Applicata*, Vol. XXXIV, No. 4, pp 573-587 (2004)
- [5] P. R. Horche, M. A. Muriel, J. A. Martín-pereda, "Measurement of Transmitted Power in Untapered Multifiber Unions: Oscillatory Spectral Behaviour", *Electronics Letters*, Vol. 25, No. 13, pp: 843-844 (1989)
- [6] Paloma R. Horche, "An Optical Multi-Bandpass Filter Obtained by Combining Bragg Reflection, Intermodal Coupling and Interference Process in an All-Fibre Device". In *proc. NOC 1998*, pp: 186-189 (1998)
- [7] Paloma R. Horche, "Measurement of the oscillatory spectral behavior of abruptly dissimilar unions fabricated with dispersion shifted fibre: Filter Application", in *proc. NOC 1996*, pp: 314-315 (1996)
- [8] Koichi Abe, Yves Lacroix, Lee Bonnell, and Zdzislaw Jakubczyk, "Modal Interference in a Short Fiber Section: Fiber Length, Splice Loss, Cutoff, and Wavelength Dependences", *Journal of lightwave technology*, VOL. 10, NO. 4, pp: 401-406 (1992)
- [9] Marco N. Petrovich, Francesco Poletti, David J. Richardson, "Analysis of Modal Interference in Photonic Bandgap Fibres", in *proc. ICTON 2010*, pp: Tu.B2.3 (2010)
- [10] Govind P. Agrawal, "Fiber-Optic communication systems", ed. John Wiley & Sons, Third edition.
- [11] Paloma R. Horche, Manuel López-Amo, Miguel A. Muriel and José A. Martín-Pereda, "Spectral Behavior of a Low-Cost All-Fiber Component Based on Untapered Multifiber Unions". *IEEE Photonics Technology Letters*, Vol 1, No 7, pp: 184-187 (1989)
- [12] Paloma R. Horche, "Transmission Properties of All-Fibre Modal Interference Devices by Fourier Transform". In *proc. NOC 1999*, pp: 317-321 (1999)
- [13] A. H. Gnauck, "40-Gb/s RZ-differential phase shift keyed transmission", in *Proc. OFC'03*, paper ThE1 (2003)